Supporting Information for

Supramolecular structure of membrane-associated polypeptides by combining solid-state NMR and Molecular Dynamics simulations

*Markus Weingarth,[†] Christian Ader,[†] Adrien J. S. Melquiond,[†] Deepak Nand,[†] Olaf Pongs,[+] Stefan Becker,[‡] Alexandre M. J. J. Bonvin[†] and Marc Baldus[†,]**

[†]Bijvoet Center for Biomolecular Research, Utrecht University, Padualaan 8, 3584 CH Utrecht, The Netherlands

[+]Institut für Neurale Signalverarbeitung, Zentrum für Molekulare Neurobiologie der Universität Hamburg, 20246 Hamburg, Germany

[‡]Department of NMR-based Structural Biology, Max Planck Institute for Biophysical Chemistry, Am Fassberg 11, 37077 Göttingen, Germany

*E-mail: m.baldus@uu.nl

This Supporting Information contains:

1. Figures S1 to S26
2. Tables S1 to S6
3. Supporting movie details
4. References

Figures

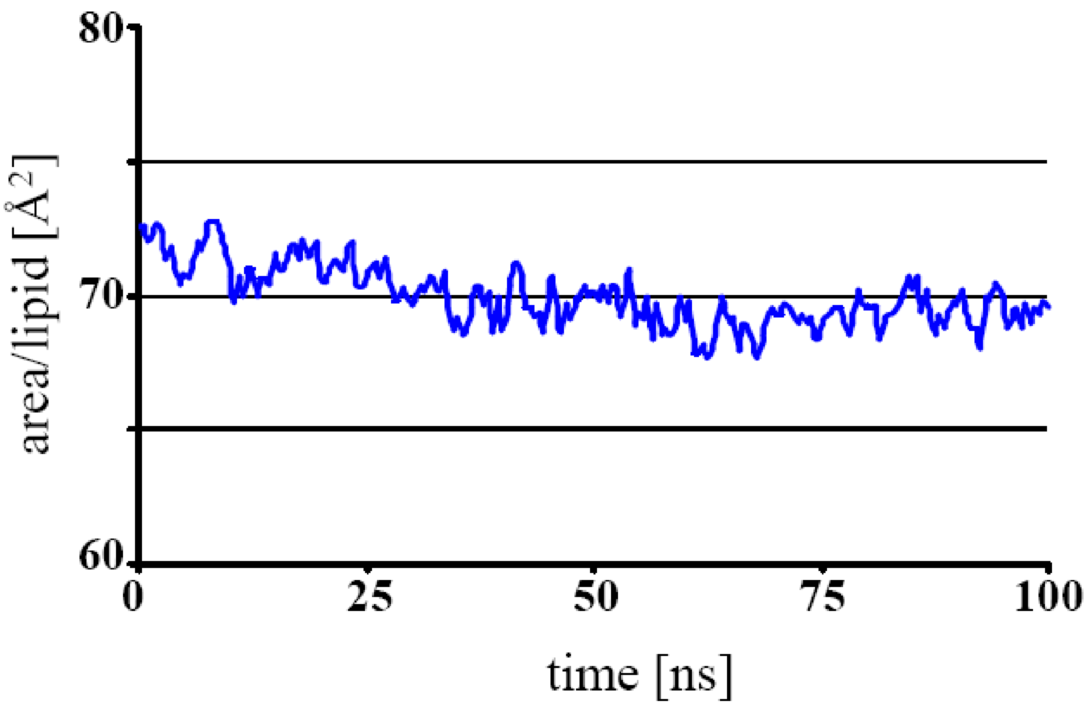

Figure S1. Time evolution of the area per lipid for the peptide-free layer of the membrane. The analyses were performed with the inflatGRO program. Note that the average value of around 69.4 ^{2} Å^{2} (averaged from 30 – 100 ns) was very close to a previous study performed by Kukol, in which an average value of 70 Å^{2} was measured after a production run of 40 ns. In Kukol's study, a POPG bilayer was simulated over 40 ns. After 40 ns, we do also observe an average value of 70 Å^{2}. Hence, the slightly different density which we obtain is very likely due to a longer simulation.

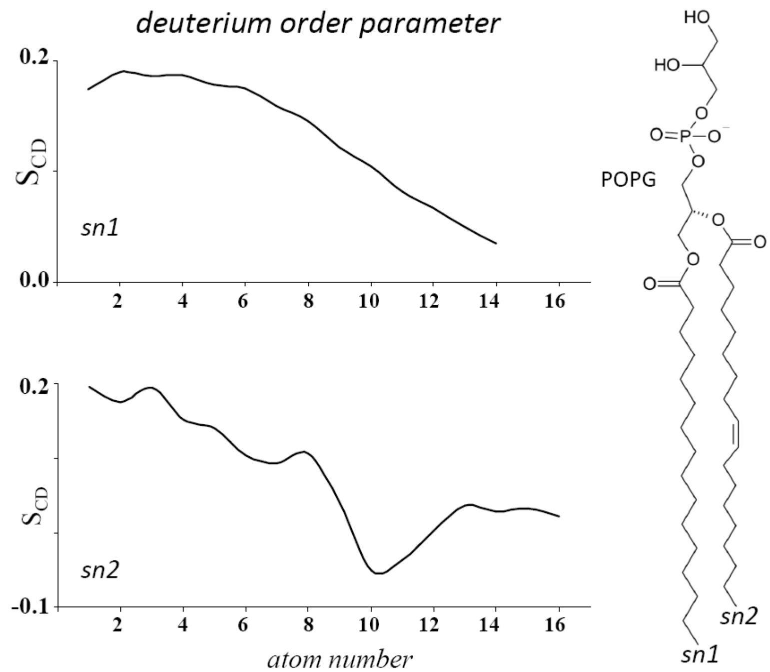

Figure S2. The deuterium order parameter S_{CD} quantifies the degree of reorientation of the lipid - acyl chains. Over the course of a MD simulation, it can be calculated as:

$$S_{CD} = \left\langle \tfrac{3}{2}\cos^2\theta - \tfrac{1}{2} \right\rangle$$

where the angle θ represents the orientation of the C-H bond vector to the bilayer normal, while the bracketing means averaging over time and all the lipids. A S_{CD} of 1 indicates a perfect alignment, a S_{CD} of 0 means a vector undergoing isotropic rotation.

Deuterium order parameters S_{CD} were averaged from a MD trajectory from 30 – 100 ns over both all *sn1* and all *sn2* chains. The saturated *sn1* and the unsaturated *sn2* lipid acyl chains are indicated in the schematic structure of POPG. Carbon 1 was defined as the carboxyl carbon in each case. The values coincide very well with the characteristic S_{CD} values for fluid phase lipid bilayers, which range from ~ 0.2 for the acyl-chain headgroups to 0 for the terminal methyl-groups (3). Moreover, the increased flexibility around atom 10 of the unsaturated *sn2* chain and the overall relative distribution of the order parameters along the acyl chains matches well with Zhao's study (4) of a POPG membrane.

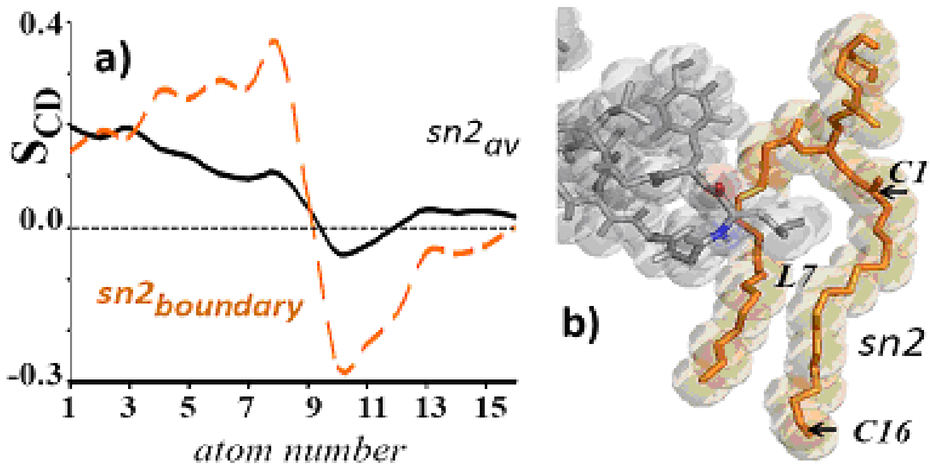

Figure S3. S_{CD} values, calculated from MD simulations, were investigated for lipid-acyl chain in direct contact with the ShB peptide ("boundary lipids"). An example for a boundary sn2 chain (orange-dashed line) is given in a) and compared to the average sn2 S_{CD} (black-continuous line). The boundary lipid features significantly restricted dynamics from C3 – C12 of sn2. b) This restrained motion is due to the lipid's interaction with the hydrophobic side chain of L7. Note that negative S_{CD} values indicate that these lipid-carbons are preferentially oriented nearly parallel to the membrane surface.

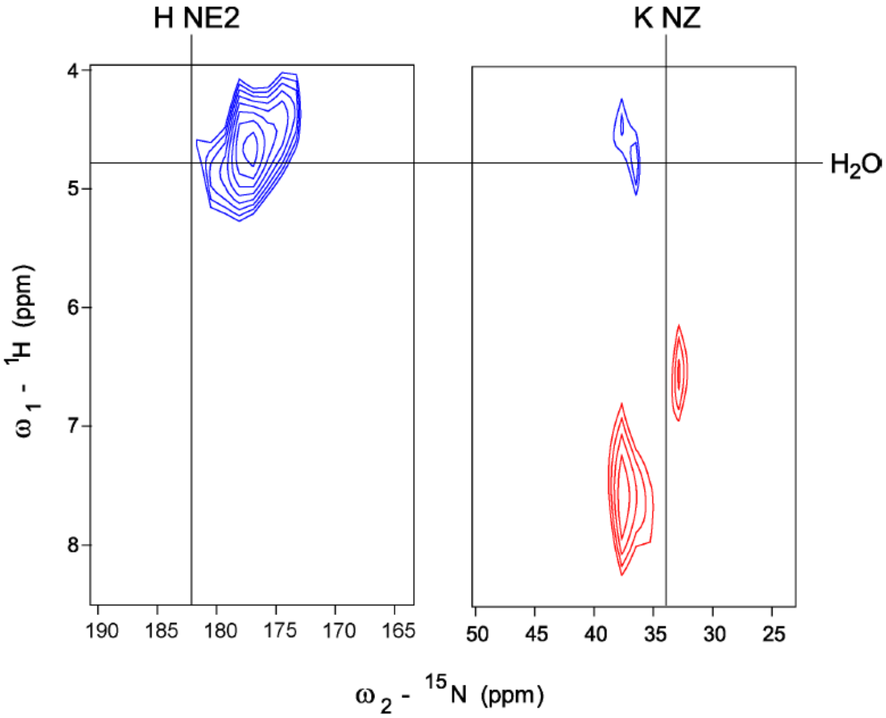

Figure S4. Water-access of lysine (K18 and K19) and histidine (H16) side chains of the membrane-bound ShB peptide. Frequency switched Lee-Goldburg (1) ^{1}H – ^{15}N correlation spectra employing no (red) and a longitudinal proton mixing time of 1 ms (blue). Average ^{15}N chemical- shifts and the water ^{1}H resonance are indicated. The C-terminal part of the ShB peptide is highly positively charged and is presumably interacting with the negatively charged lipids, as the MD simulations also showed. Yet, the interactions between the positively charged side chains of lysine or histidine and the polar lipid functions do not persist for more than a few ns, which indicates why we observed only some resonances of the mobile C-terminus in spin diffusion spectra.

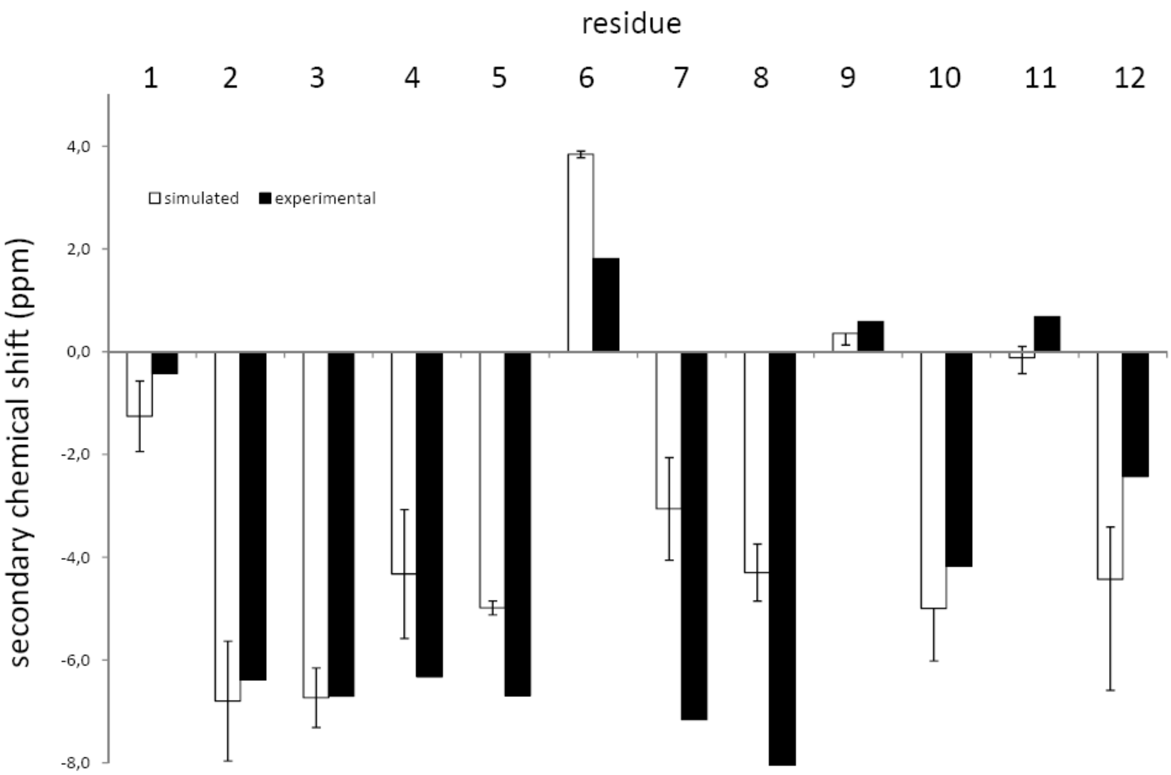

Figure S5. Secondary chemical-shifts computed on the basis of the experimental chemical-shift assignment of the ShB peptide (black) and ShiftX (2) chemical-shift predictions obtained for the 20 lowest energy structures of the ShB peptide (white, standard deviations for the 20 evaluated structures are indicated).

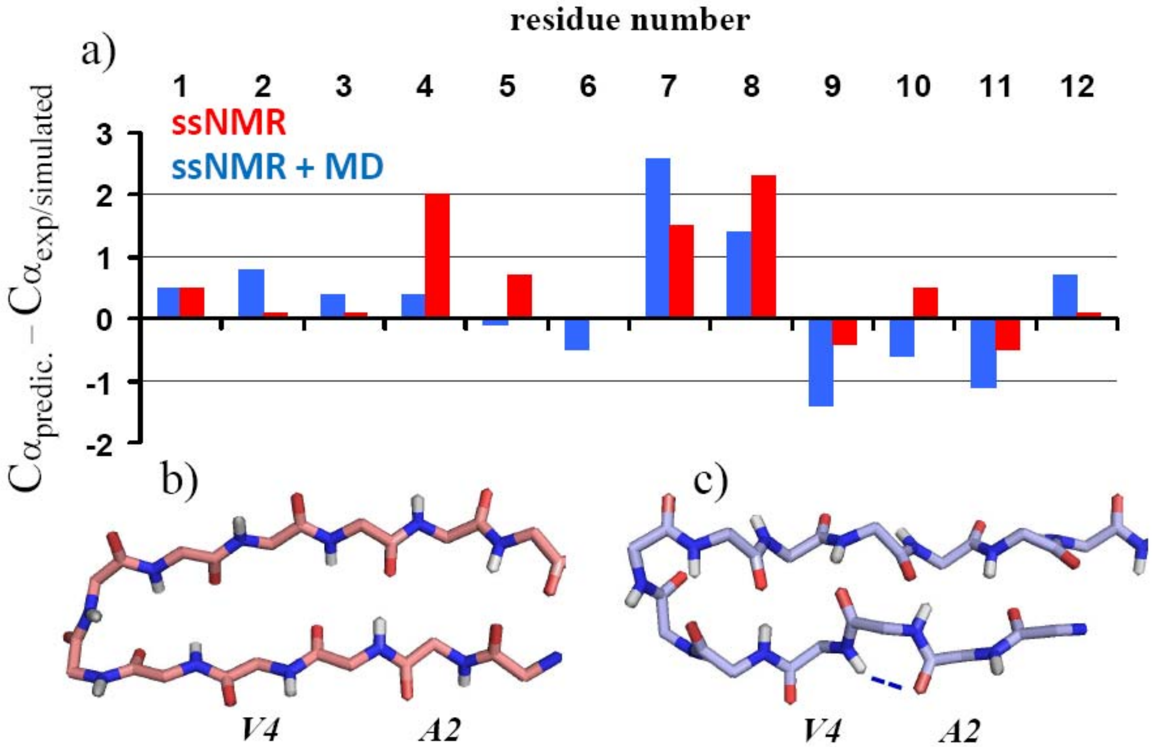

Figure S6. a) Cα chemical-shift differences calculated as $\Delta_{CS} = CS_{predicited} - CS_{ssNMR}$ and $\Delta_{CS} = CS_{predicited} - CS_{ssNMR+MD}$, respectively. b), c) Structures of the ShB peptide obtained by b) ssNMR and c) ssNMR + MD. Note that V4Cα of c) is much closer to the prediction than b) due to an intra-peptide hydrogen bond between A2NH - V4Hα. All chemical-shifts were predicted with the SPARTA$^+$ software.

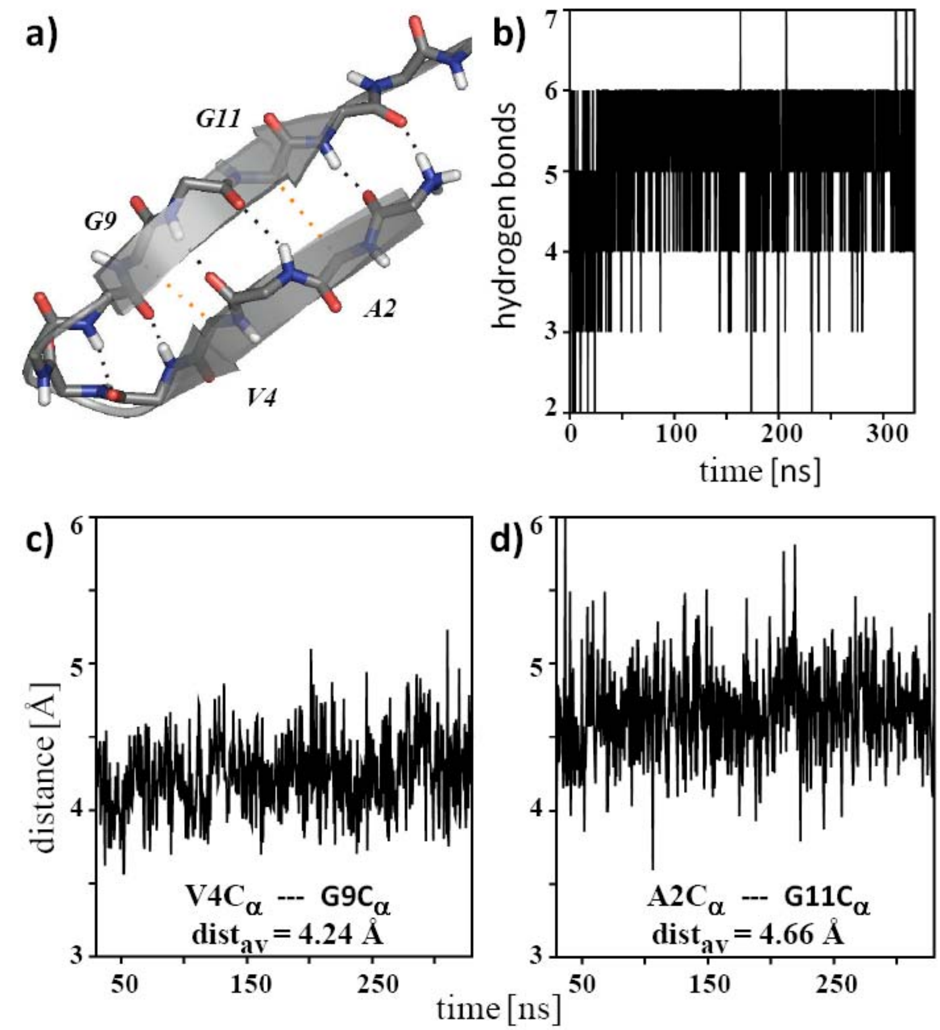

Figure S7. a) The total number of inter-β-strand hydrogen bonds between residues M1 --- E12, A3 --- L10 and A5 --- Y8 and inter-β-strand distances V4Cα --- G9Cα and A2Cα --- G11Cα were evaluated from a simulation of the monomeric membrane-bound ShB peptide using the ssNMR ShB peptide structure and topology as starting point. Hydrogen bonds and carbon - carbon distances are indicated as blue and brown dashes, respectively. The snapshot of the peptide backbone was taken after 48 ns. b) The average number of inter-β-strand hydrogen bonds, measured from 30 to 330 ns. The total number of inter-β-strand hydrogen bonds. was 5.25. The distances c) V4Cα --- G9Cα and d) A2Cα --- G11Cα fluctuated smoothly around their average distances 4.1 Å and 4.5 Å, respectively. This is in good agreement with PDSD-WC (Proton-driven spin diffusion weak coupling condition) and ^{13}C-^{13}C PARIS-xy (Phase-alternated recoupling irradiation scheme using orthogonal radio-frequency phases) experiments, which indicated long-range contacts between these carbons.

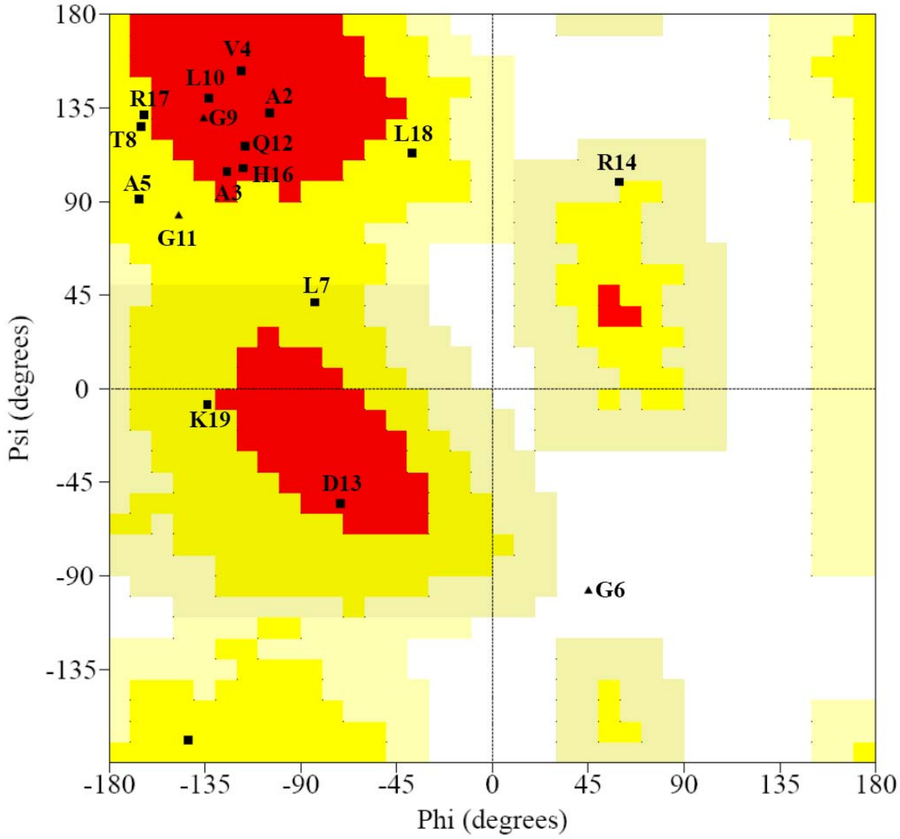

Figure S8. Ramachandran plot averaged over a 30 ns free simulation of the membrane-bound ShB monomer system. Non-glycine residues are marked as squares, glycines as triangles. The most favorable regions for generic (non-proline, non-glycine) residues are coloured in red, additional allowed regions in yellow and generously allowed regions in cream. In total, eight residues are in most favorable regions, nine residues in additional allowed regions and one in generously allowed regions. For the glycine, the colour scheme is different and residue six is situated in an allowed region.

The plot matches well with residues 1 - 12 forming a β-hairpin. Indeed, residues 2-4, 9-10 and 12 are in the most favourable region for β-hairpins, while residues 5, 8 and 11 are in additional allowed regions. Note that according to the MD simulations and NHHC experiments, the dihedral angles of residues 6 and seven 7 indicate rather a type II' β-turn that a type VIII β-turn. For both types of turns, the positive secondary chemical-shift of G6 and the negative secondary chemical-shift of L7 are consistent (Figure S5).

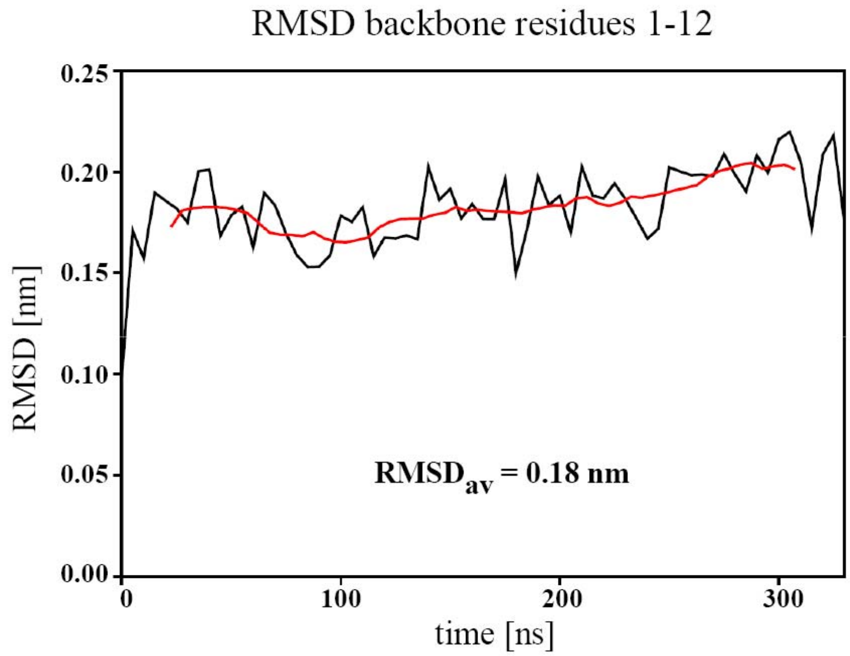

Figure S9. RMSD of the peptide backbone of residues 1 - 12 with respect to the ssNMR structure. The RMSD was calculated every 5 ns over a total trajectory of 330 ns. A running average is shown in red.

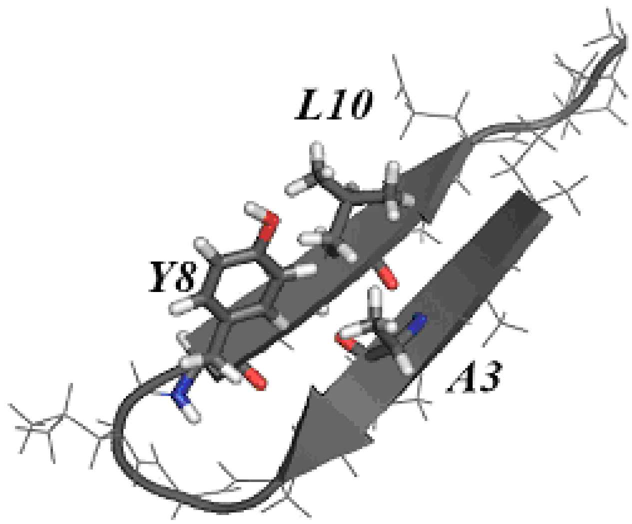

Figure S10. PARIS-xy experiments were prompted by the observation that the hydrophobic side chains of A3, 8Y and L10 oriented preferentially close to each other over the course of the MD trajectory.

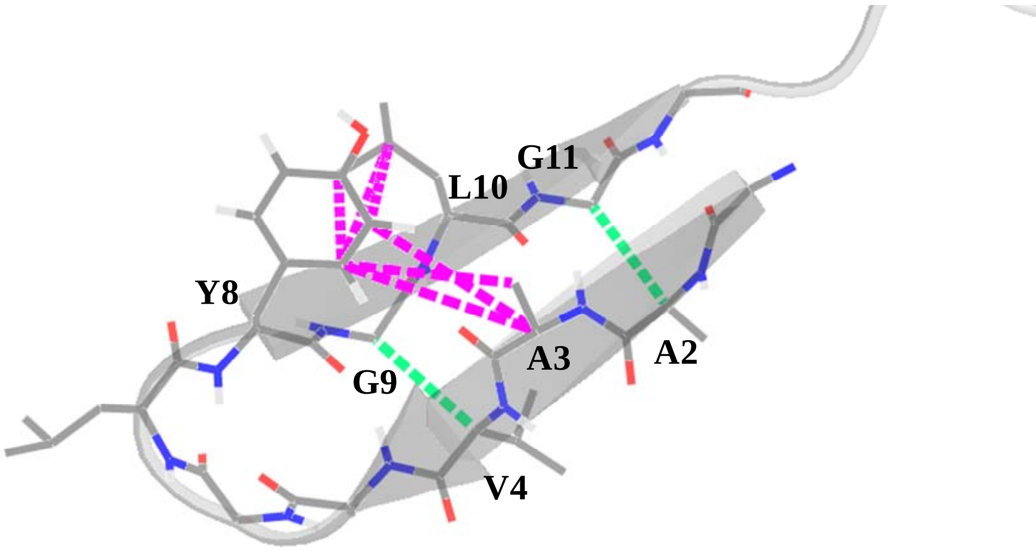

Figure S11. The inter-residual contacts between residues A2 – G11 and V4 – G9 which we detected in the first round of ssNMR, are highlighted in green (two additional proton-proton contacts are not shown for clarity). The inter-residual and inter-strand molecular contacts which we observed by tailored, chemical shift selective ssNMR (rotational resonance recoupling and PARIS-xy are highlighted in magenta (contacts in the range from 3.8 – 5.0 Å). The network of ssNMR long-range contacts confirms our structure and validates the MD simulations. The Figure shows the ssNMR-MD structure after 120 ns of free simulation.

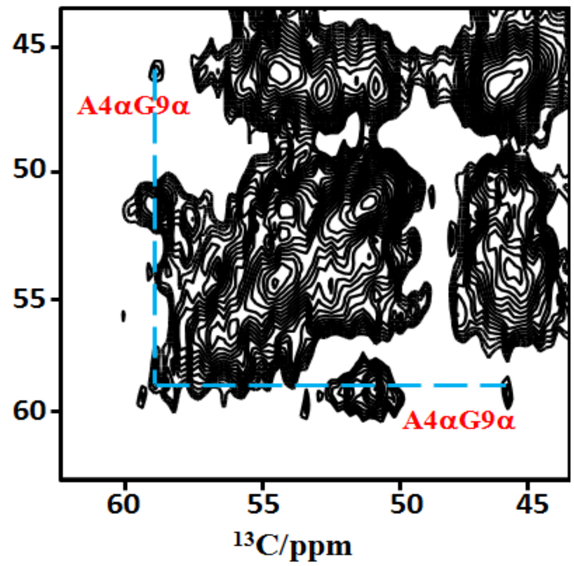

Figure S12. A PARIS-xy ^{13}C-^{13}C spin diffusion experiment (*m* = 2, recoupling amplitude 10 kHz, 250 ms mixing time) confirmed the presence of the proximity of residues V4-G9 expected for the β-hairpin structure of the ShB peptide discussed in the main text (Figure 1e).

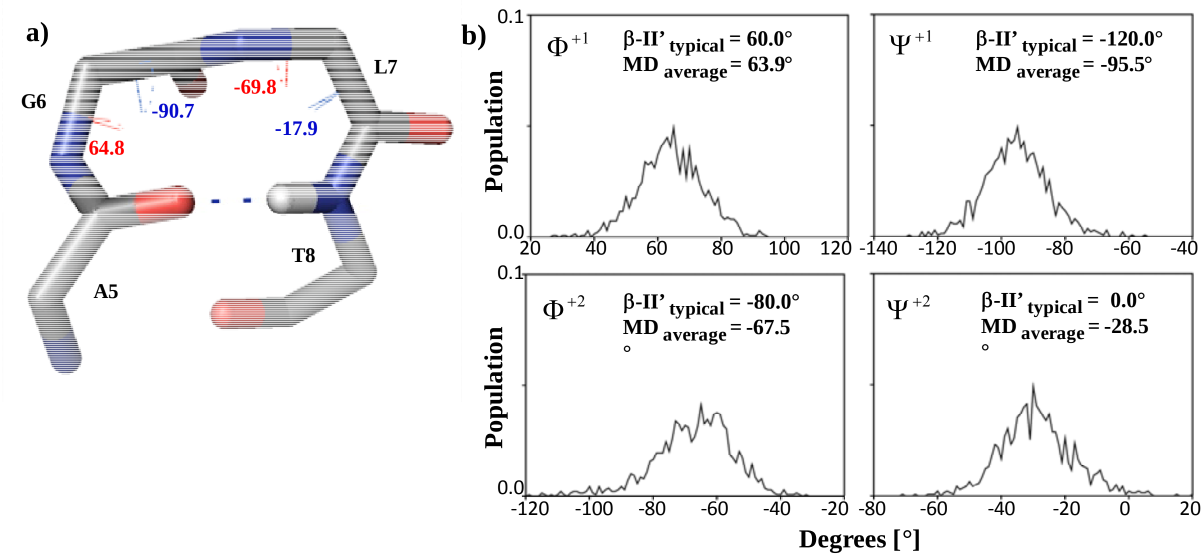

Figure S13. a), b) The β-turn formed by the peptide residues 5 - 8 changed over the course of the MD trajectory swiftly (within less than 1 ns) from turn type VIII turn to type II' turn. Snapshot a) was taken after 48 ns of a production run. Dihedral angles were measured from 30 – 330 ns.

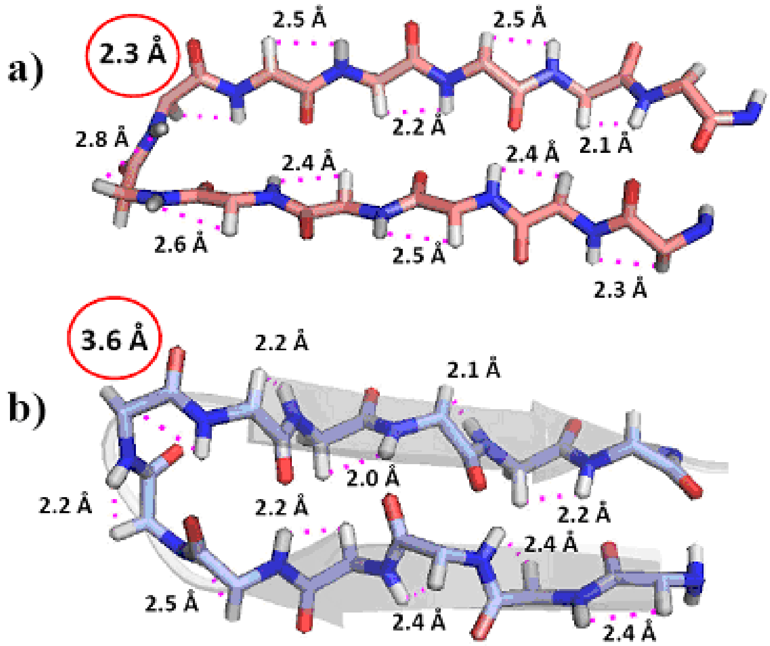

Figure S14. Comparison of the structures of the ShB peptide as seen by a) ssNMR (featuring type VIII turn) and b) ssNMR – MD (featuring type II' turn). While in a) all sequential NH^{i} – $H\alpha^{i-1}$ contacts are in the range of 2.2 – 2.8 Å, the ssNMR - MD structure shows one remarkable exception with 8YNH – 7LHα, which features a distinctively longer distance between 3.3 – 3.7 Å. Since we could not detect the 8YNH – 7LHα contact by NHHC experiments, type II' turn is experimentally corroborated. Notably, despite the ssNMR - MD structure looking partially slightly disordered, the dihedral angles match better with a β-hairpin than the ssNMR structure (Figure 2 of the main text).

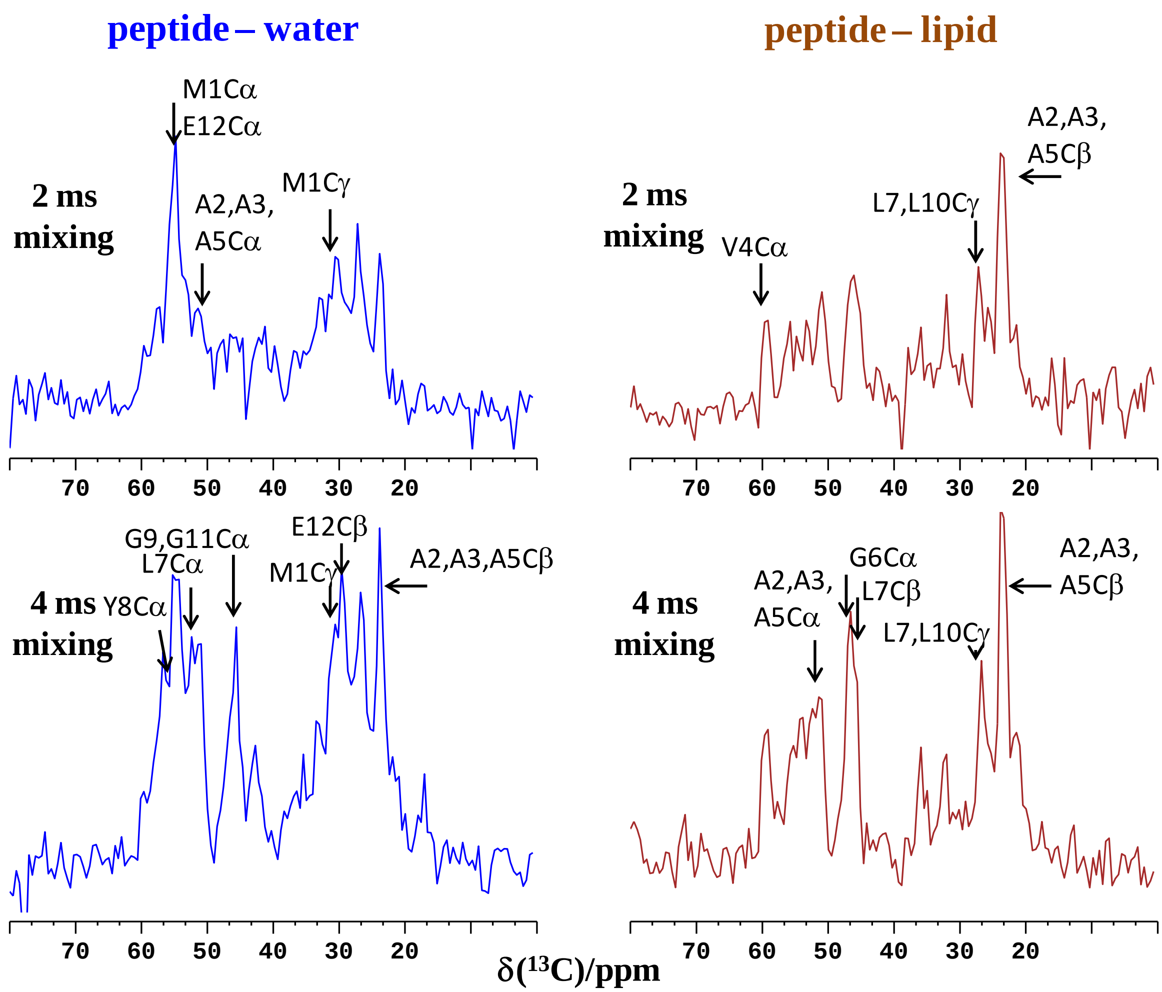

Figure S15. ^{13}C cross sections at the water ^{1}H chemical shift (left) and the lipid chain ^{1}H signal (right) of T_2-edited 2D HHC experiments with 2 and 4 ms mixing time, respectively. Each 2D spectrum was measured with 1344 scans and an evolution time of 2 ms in the indirect dimension.

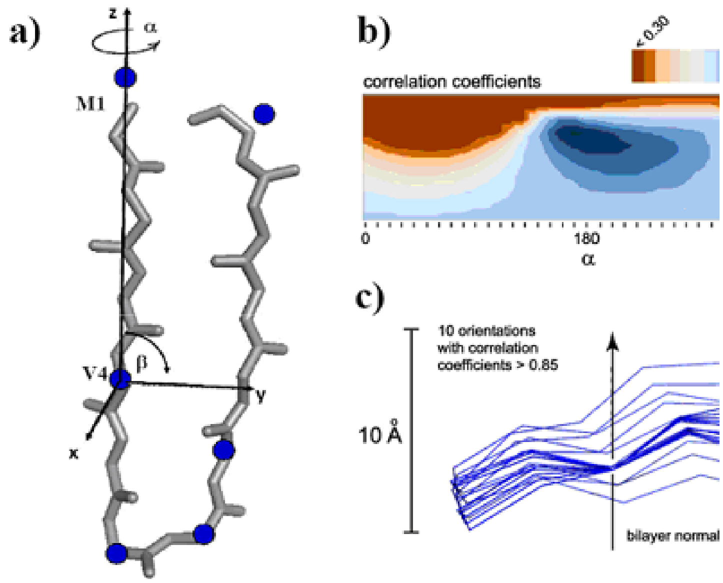

Figure S16. Approximating the membrane topology of the membrane-bound ShB peptide on the basis of water – protein and lipid – protein exchange rates. a) Backbone representation of the ShB β-hairpin (residues 1 - 12, black). Atoms for which site resolved exchange rates were obtained are indicated as blue spheres. The molecule is positioned in a coordinate system such that the atom characterized by the smallest ratio of water – protein and lipid – protein rates (V4 Cα) is located in the origin and the atom attributed to the largest absolute ratio (M1 Cγ) lies on the z axis which represents the bilayers normal. Possible orientations of the peptide with respect to the bilayers normal are sampled by performing independent rotations around z (angle α, $0 \leq \alpha \leq 350$) and x (angle β, $0 \leq \beta \leq 90$) in 10 degree increments. The z coordinates of the considered atoms in direction of the bilayer normal then are measures for the orientation of the atoms with respect to the water – bilayer interface. b) Contour plot for the correlation coefficients computed between the relative localization of the atoms along the bilayer normal and their respective ratio of water – protein and lipid – protein rates as a function of the angles α and β. Increasing correlation is indicated by a color gradient from dark red to dark blue. c) Ensemble of 10 membrane topologies of the ShB peptide agreeing best with the measured water – protein and lipid – protein magnetization transfer rates (exhibiting correlation coefficients larger than 0.85). The bilayer normal and a scale bar are indicated.

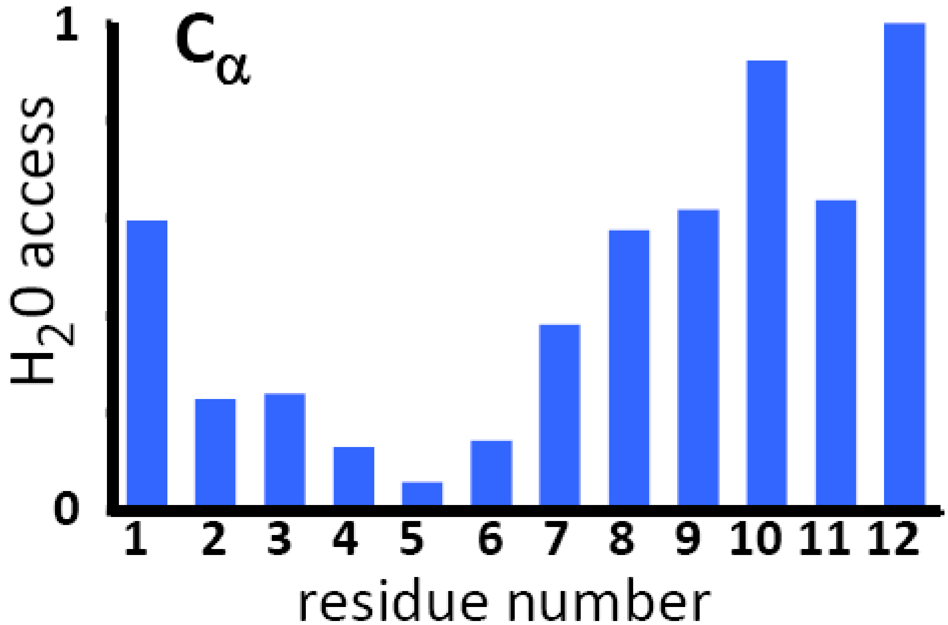

Figure S17. The water-access of the Cα of the peptide residues 1 - 12 back-calculated from a MD simulation. The number of water molecules was averaged from 30 – 330 ns within a radius of 9 Å.

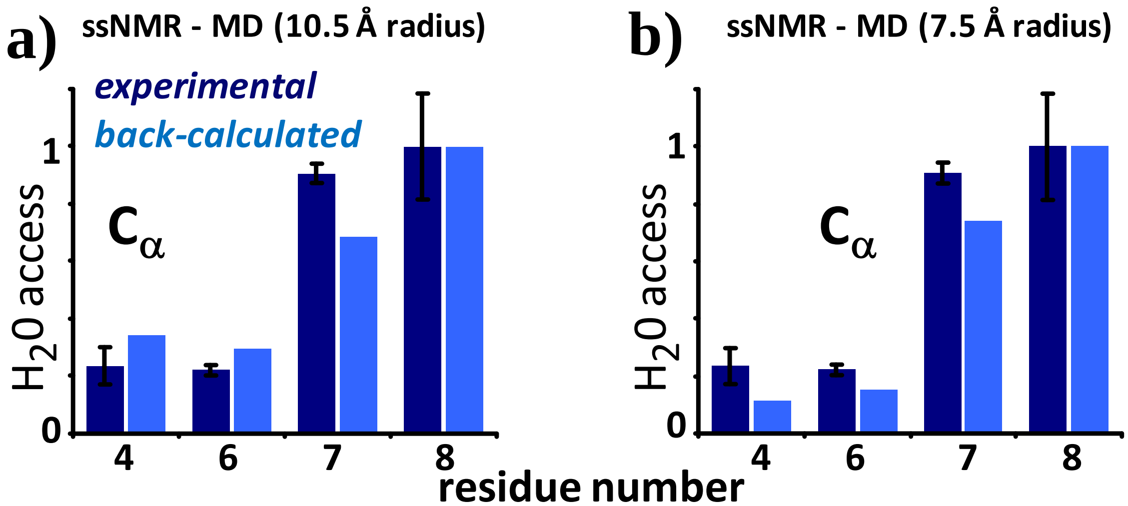

Figure S18. The agreement of experimental and back-calculated water-access for the ssNMR – MD structure and topology does not depend much on choice of the radius within which water-molecules were averaged over the course of the trajectory. While the agreement is quantitatively very good for a radius of 9 Å (see Figure 4 of the main text), the agreement is very good for a) larger radii and b) still reasonable for smaller radii. All these radii allow deducing that the plane of the β–hairpin formed by the ShB peptide needs to be inclined with respect to the bilayer normal. The water-access averaged from 30 – 330 ns.

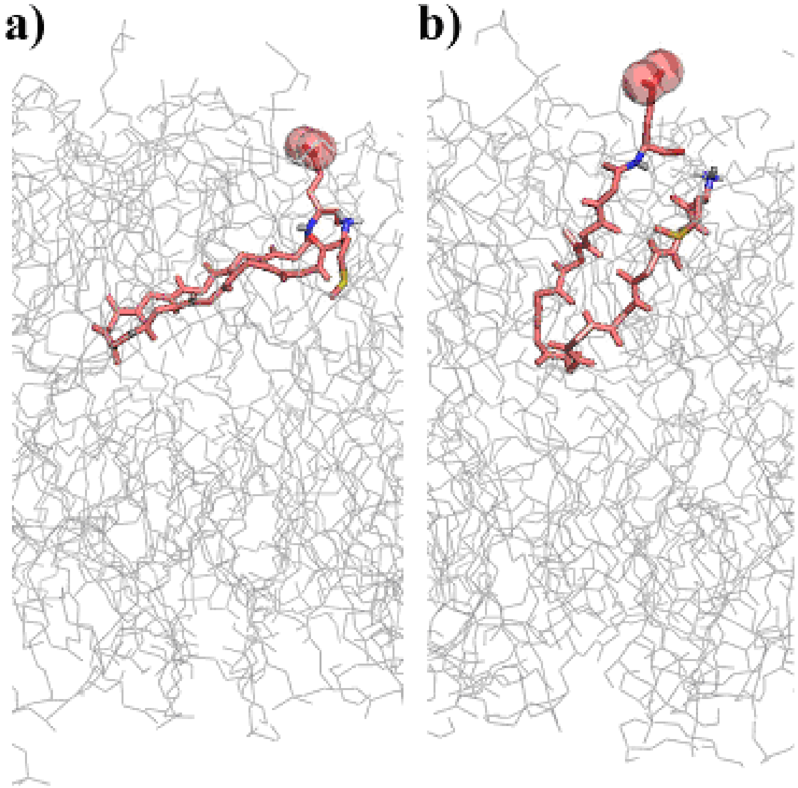

Figure S19. a) To examine the insertion depth of the ShB peptide**,** the ssNMR structure was placed 7 Å deeper along the bilayer normal as suggested by the T_2 edited HHC experiments. b) The ShB peptide reoriented within 10 ns in adopting a much smaller tilt (see Figure S20), so that residues M1 and the negatively charged E12, in particular, retrieved the bilayer - water interface, just as suggested by the experimental data. The oxygen–atoms of the carboxyl–groups of E12 are highlighted as spheres.

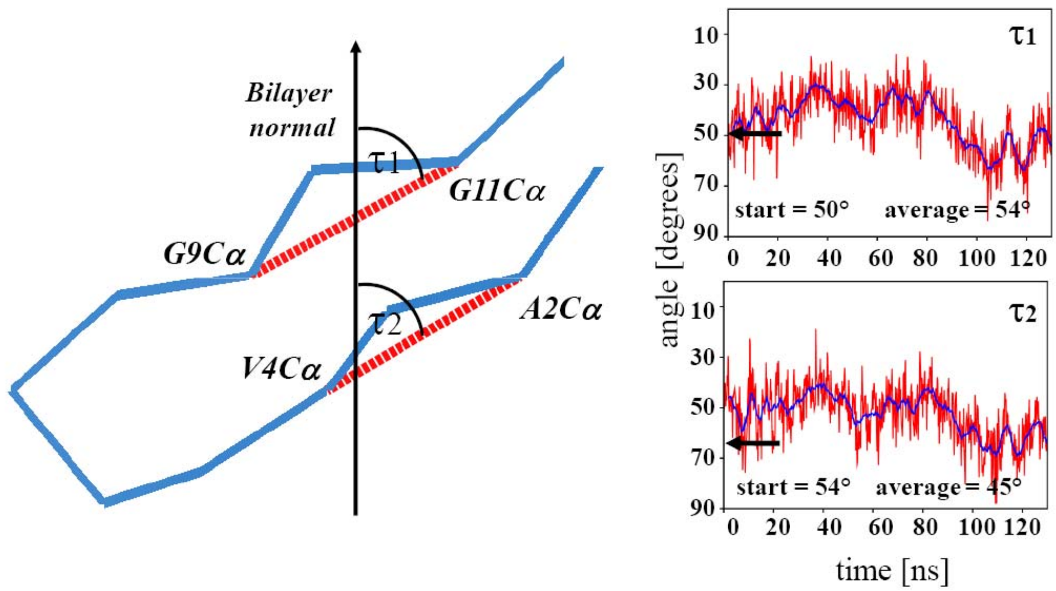

Figure S20. The β-strand tilt angles τ1 and τ2 are between the bilayer normal and the vector G11Cα-G9Cα and A2Cα-V4Cα, respectively. The β-strand tilt angle τ is the average of these two angles. Angles were evaluated every 200 ps (red lines). The blue lines show running averages and the black arrows indicate the orientation at the beginning of the trajectory.

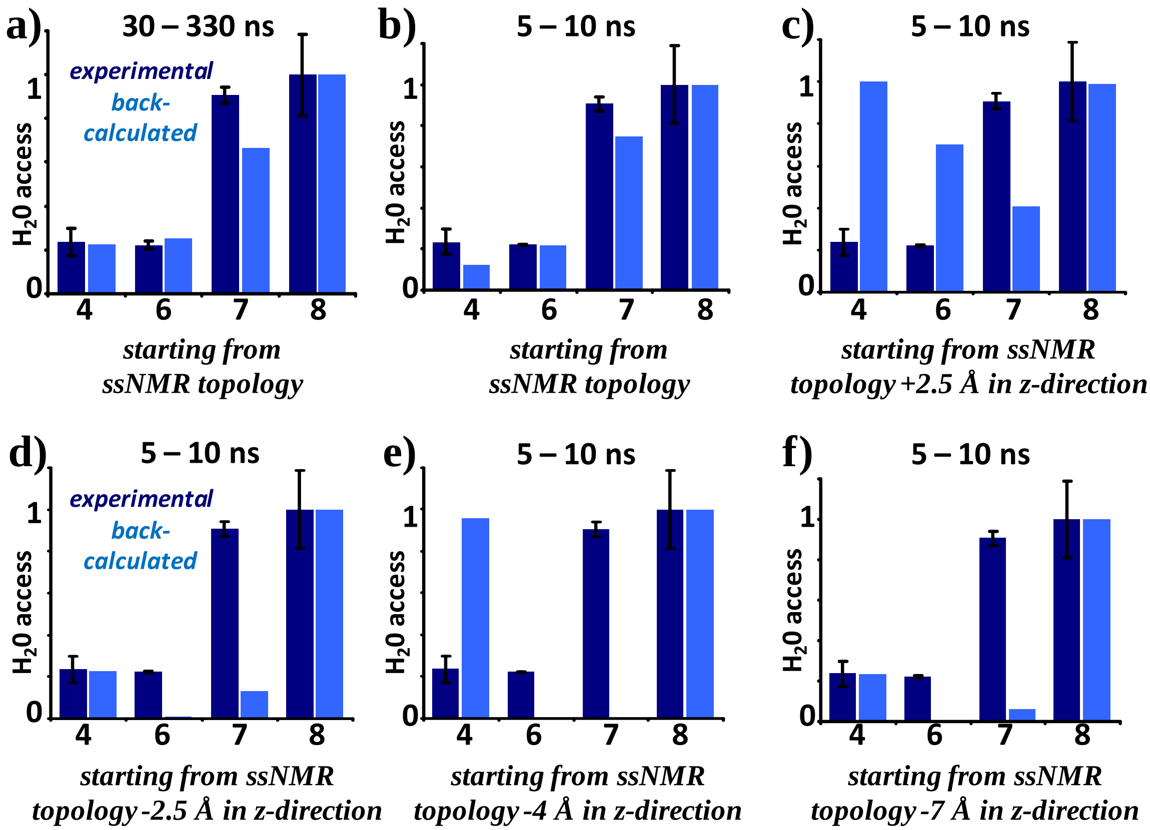

Figure S21. Comparison of the peptide's water-access obtained with T_2 edited HHC experiments (dark blue columns) and the water-access back-calculated from MD simulations (light blue columns) for some resolved Cα resonances. As starting structures for the MD simulations, we either used a), b) the unmodified ssNMR topology or c)-f) the ssNMR topology with the ShB peptide shifted by +2.5, -2.5, -4 and -7 Å along the bilayer normal (corresponding to the z axis), respectively. For the MD-simulations, the number of water molecules was averaged from a) 30 – 330 and b) – f) 5 – 10 ns. It is obvious from the data that the back-calculated water-access matches much better with the original ssNMR topology as starting structure. Longer sampling times were not possible for some of the modified starting structures because the β-hairpin either became partly unstructured or the peptide inserted very deep into the membrane. This again highlights that a good starting structure is pivotal to proper interpretation of MD simulations of the membrane-bound systems.

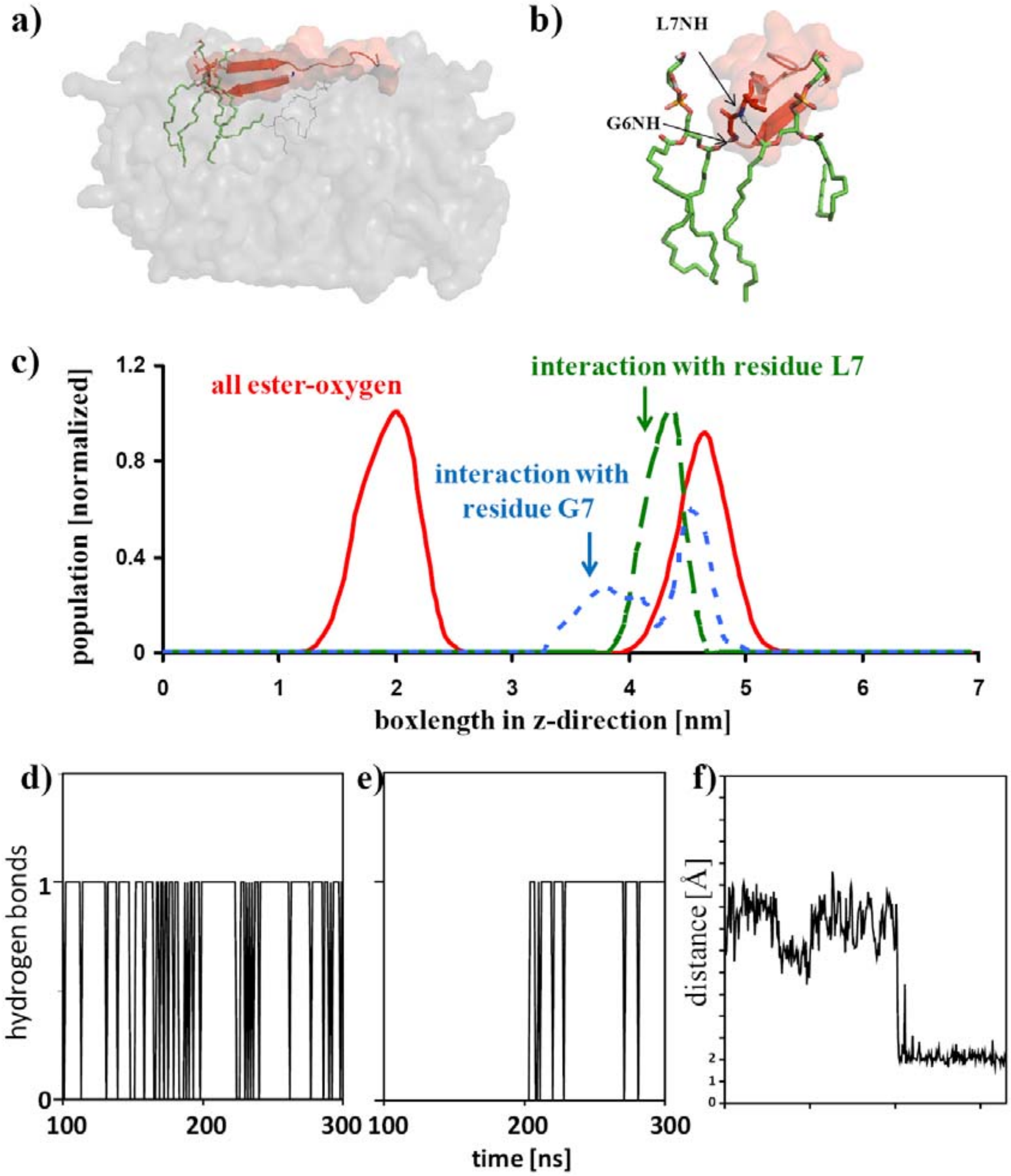

Figure S22. To enable lipid-peptide hydrogen bonds with lipid-ester groups or lipid-phosphate-functions, the membrane width is locally reduced around the membrane-inserted ShB peptide residues, which is deducible from some lipid-ester functions residing distinctly deeper in the membrane. a) A snapshot taken after about 300 ns of MD simulation. b) Zoom of a). Two lipid molecules reside particularly deeply within the membrane to form hydrogen bonds with the polar NH-functions of G6 and L7. The amino-functions do not take part in the intra-peptide hydrogen-bonding pattern and are saturated by hydrogen-bonds with deeply within the membrane residing lipid-ester-functions. These hydrogen-bonds are strong (distance NH ---- O between 1.8 and 2.5 Å) and very stable (hydrogen bond with G6NH and L7NH formed after ~ 50 and 200 ns, respectively) and persisted till the end of the trajectory of 330 ns. The strong lipid interaction which G6NH and L7NH are involved in may also explain why the back-calculated chemical shift of L7Cα of the ssNMR-MD structure deviated from the experimental chemical shift. Such lipid-peptide contacts are not taken into account by current chemical shift prediction algorithms. c) The bilayer width is locally reduced around the ShB peptide to enable hydrogen bonds between peptide and lipid ester- and phosphate-groups (black spheres). In the simulations, lipid molecules (highlighted in a) and b) moved very deep into to bilayer to enable hydrogen bonds with the backbones of G6, L7 and G9. The average density profile of POPG phosphate-groups is shown in red continuous lines, the profile of lipids interacting with G6 and L7 in blue short dashed and green long-dashed lines, respectively. Profiles are normalized. d,e) The peptide-lipid hydrogen bonds involving d) G6NH and e) L7NH over time. f) The lipid-peptide hydrogen bonds are very strong. The distance between the amino-proton of L7 and the lipid ester oxygen (which is the hydrogen- bond acceptor) is shown as an example. The average distance from 220 – 330 ns is 2.09 Å.

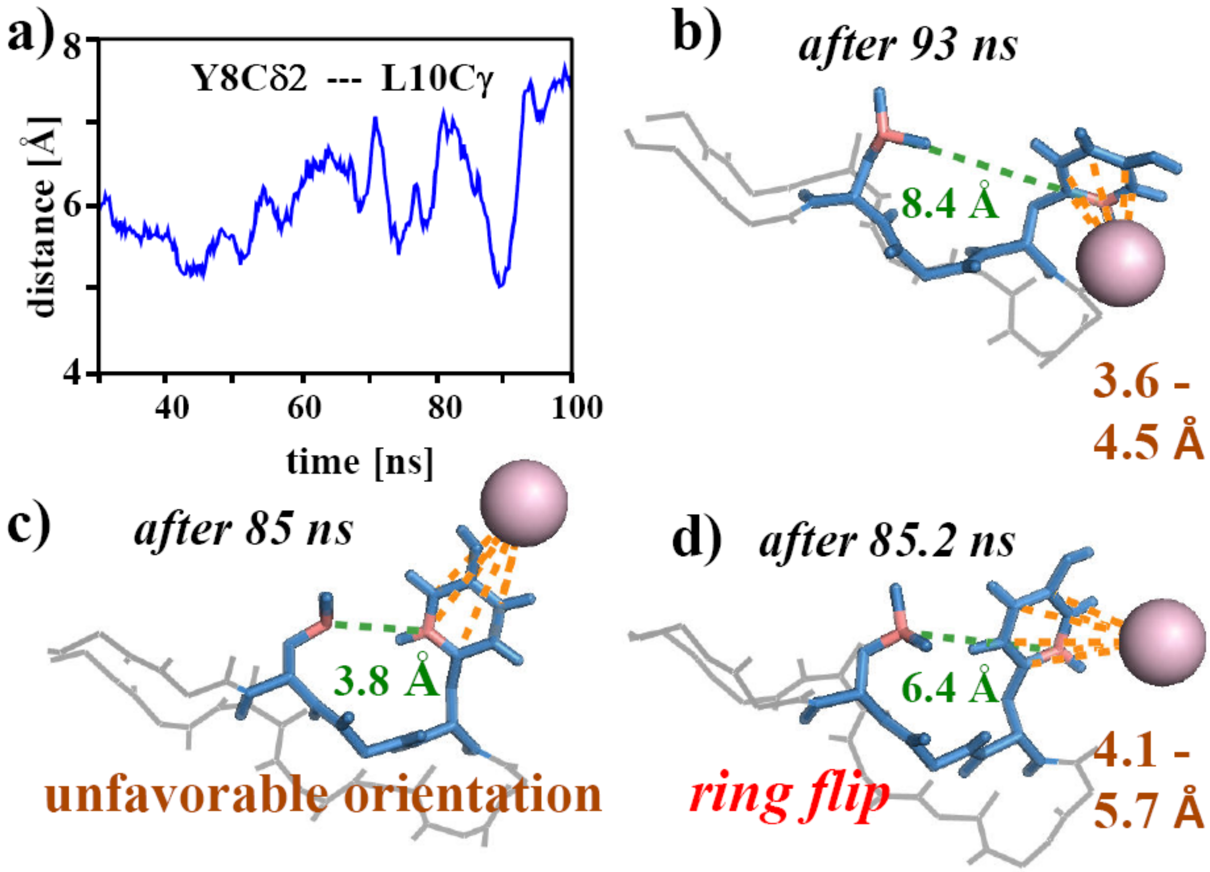

Figure S23. The MD simulations showed that the aromatic moiety of Y8 is involved in cation-π interaction and featured two distinct conformations with the edge and the center of the aromatic ring turned towards the side chain of L10, a) exemplified on the distance Y8Cδ2 --- L10γ. b-d) The driving force of the alternating ring conformations was a cation-π interaction, which established after about 60 ns, imposing the edge conformation and inducing ring-flips. Not all shown states are resolved in a), since the running average is shown.

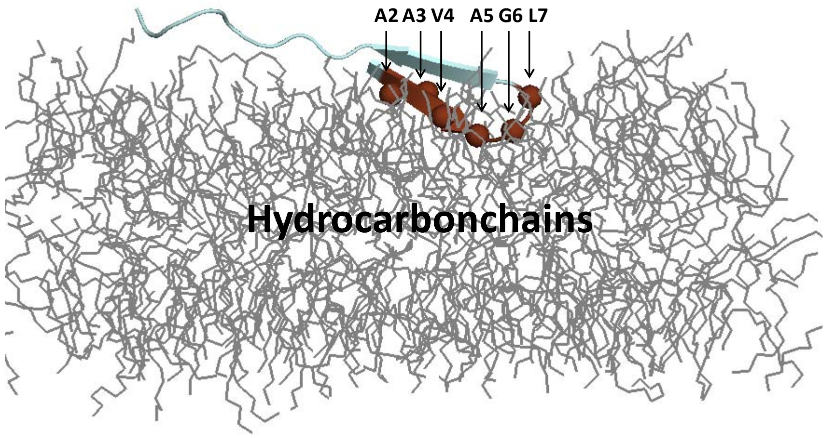

Figure S24. A snapshot taken after about 300 ns of free MD simulation of membrane-bound ShB peptide. Only the hydrocarbonchains of the bilayer are shown. Residues A2-L7, which showed relatively strong lipid-protein cross-peaks in T_2-edited HHC experiments, are colored in brown. The $C\alpha$ atoms of residues A2-L7 are highlighted as spheres.

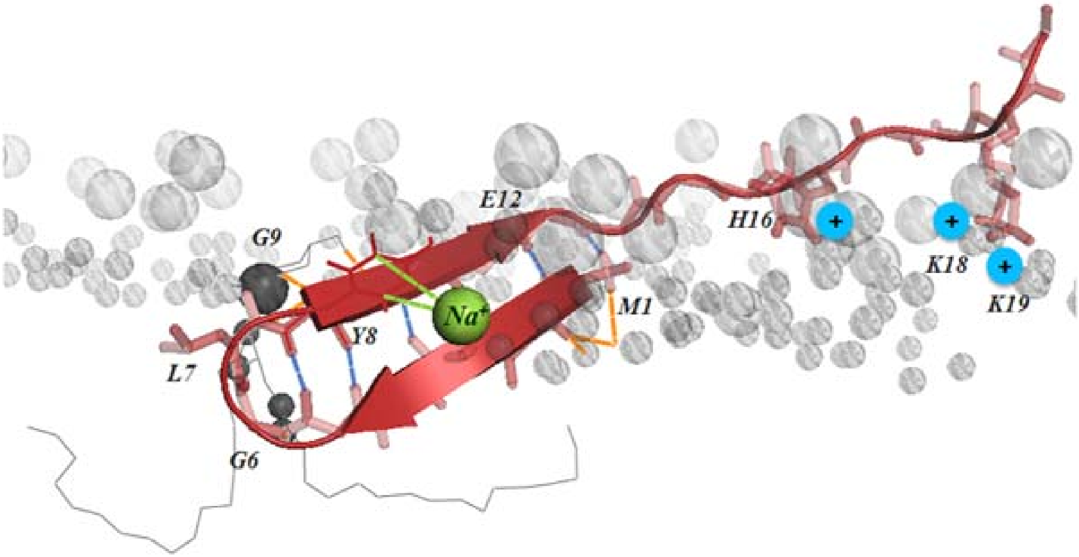

Figure S25. The supramolecular structure of the membrane-bound ShB peptide, from different a perspective to Figure 5 of the main text (after 130 ns). The hydrophobic side chain of L7, pointing towards the bilayer hydrophobic core, was demonstrated to be crucial for the insertion of the ShB peptide into lipid bilayers. Moreover, a ShB-L7E mutant showed reduced binding affinity to the KcsA channel and was unable to adopt β-hairpin configuration.

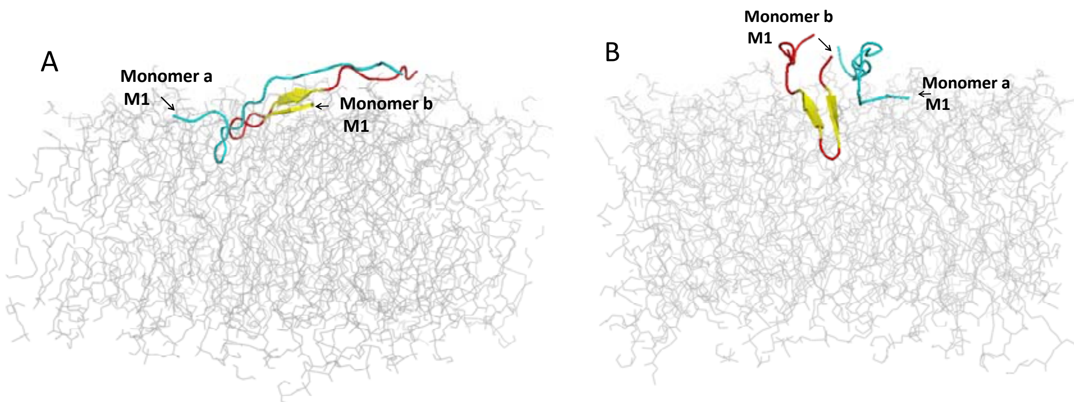

Figure S26. Two simulations with two different membrane-bound dimeric ShB peptide starting structures were evaluated. **(A)** For the first starting structure, two ssNMR structures with the topology obtained with T_2 edited HHC experiments were placed next to each other with a shift of 1 nm so that they could form a larger 4 strand β−sheet. **(B)** For the second starting structure, we placed two peptides with the ssNMR - MD structures and topologies next to each other. Yet, in both cases at least one of the peptides did not show an extended secondary structure. Such a distorted construct is not in accordance with the ssNMR chemical shifts. Structural distortions are induced by inter-peptide polar contacts and hydrogen bonds. In (A), an inter-peptide interaction between the C-terminal tails was observed. Hence, the simulations suggest that the proximity of the two peptides precludes the formation of a β-hairpin that is significantly inclined with respect to the bilayer surface. Yet, only such an orientation is in accordance with our water-edited data. Snapshots were taken after (A) 50 ns and (B) 10 ns of free simulation.

Tables

Table S1. Experimental details on 2D ssNMR spectra obtained for the uniformly (^{13}C, ^{15}N) labeled ShB peptide bound to DOPC/Cardiolipin liposomes.

Spectrum	^{1}H frequency	MAS	Mixing	CP contact times	TD1	NS	D1	time
PDSD	700 MHz	13 kHz	20 ms	700 µs	230	96	2 s	12 h
PDSD-WC	700 MHz	10.9 kHz	200 ms	700 µs	230	176	2 s	23 h
SPECIFIC NCA	700 MHz	13 kHz	-	500 µs/ 3 ms	32	704	2 s	13 h
SPECIFIC NCOCX	700 MHz	13 kHz	30 ms	500 µs/ 3 ms	24	1920	2 s	26 h
CHHC	700 MHz	13 kHz	500 µs	700/120/120 µs	96	1760	2 s	4 d
NHHC	700 MHz	13 kHz	150 µs	600/250/150 µs	38	4288	2 s	4 d
T_2 filtered HHC	500 MHz	10 kHz	0 - 4 ms	150 µs	20	1344	2 s	15 h
PARIS-xy	500 MHz	13.8 kHz	250 ms	850 µs	190	700	2.1 s	3d 13 h

Mixing times refer to ^{1}H – ^{1}H and ^{13}C – ^{13}C longitudinal mixing times. Cross polarization (CP) contact times are stated in order of occurrence in the respective experiment. Furthermore, the number of data points in the indirect dimension (TD1), the number of scans per t1 increment (NS), and the repetition delay (D1) as well as the total acquisition times (time) are listed.

Tables

Table S2. Spectral assignment of uniformly (^{13}C, ^{15}N) labeled ShB peptide in DOPC/Cardiolipin membranes under Magic Angle Spinning (in ppm).

Residue		Cα	Cβ	C'	N	Cγ(1)	Cδ1	Cγ(2)	Cε
1	M	54.8	32.3	-	-	30.7			17.2
2	A	51.2	23.5	175.1	123.4				
3	A	51.1	23.6	175.4	120.7				
4	V	59.5	35.9	172.6	115.8	21.2			
5	A	51.2	23.6	176.0	124.1				
6	G	47.2		169.7	106.4				
7	L	52.9	46.8	173.4	116.1	26.8	23.2	23.2	
8	Y	55.7	46.8	175.2	116.4				
9	G	46.0		170.5	104.7				
10	L	54.7	45.7	175.3	119.5	26.6	23.7	23.7	
11	G	46.1		170.6	104.9				
12	E	54.6	29.8	171.7	122.4	34.0	180.0		

Table S3. Distance constraints obtained for the membrane-bound ShB peptide by ssNMR spectroscopy.

Distance constraints			
NHHC (150 μs proton mixing time)			
A2 HN	-	M1 Hα	
A3 HN	-	A2 Hα	*
V4 HN	-	A3 Hα	
A5 HN	-	V4 Hα	
G6 HN	-	A5 Hα	
L7 HN	-	G6 Hα	
G9 HN	-	Y8 Hα	
L10 HN	-	G9 Hα	
E12 HN	-	G11 Hα	
CHHC (500 μs proton mixing time)			
A2 Hα	-	G11 Hα	
V4 Hα	-	G9 Hα	
PDSD-WC (200 ms carbon mixing time)			
A2 Cα	-	G11 Cα	

* ambiguous due to overlap with intra-residue cross peaks

Table S4. Structural constraints used for the ssNMR structure determination of the membrane-bound ShB peptide in CNS.

Distance constraints	Total	^{1}H - ^{1}H	^{13}C - ^{13}C
Total	13		
Sequential (|i-j| = 1)	9	9	-
Long range (|i-j| > 1)	4	2	2
Dihedral angles restraints			
Total	22		
TALOS	18		
Turn analysis*	4		
Hydrogen bond restraints			
Total	4		

*based on secondary chemical-shift analysis

Table S5. Stereochemical quality parameters and energy statistics for the structure of the membrane-bound ShB peptide.

Average RMSD to mean coordinates*	20 lowest energy structures	
Backbone heavy atoms	0.43 ± 0.18	Å
All heavy atoms	1.35 ± 0.25	Å
Ramachandran analysis*(5)	**20 lowest energy structures**	
Most favored regions	71.4	%
Additional allowed regions	28.6	%
Generously allowed regions	0.0	%
Disallowed regions	0.0	%
CNS energy statistics**	**20 lowest energy structures**	
Overall	17.4 ± 0.1	kcal mol^{-1}
Bonds	0.22 ± 0.01	kcal mol^{-1}
Angles	13.63 ± 0.03	kcal mol^{-1}
Impropers	0.62 ± 0.01	kcal mol^{-1}
Van der Waals	2.13 ± 0.06	kcal mol^{-1}
Distance constraints	0.08 ± 0.01	kcal mol^{-1}
Dihedral constraints	0.70 ± 0.02	kcal mol^{-1}

* determined for residues M1-E12

** determined for residues M1-Q20

Table S6. Structural constraints which were added to those listed in Table S3 for a second run of CNS structure determination of the membrane-bound ShB peptide. These restraints were either directly extracted from the MD trajectory (the hydrogen bond/polar contract restraint) or prompted by observation of the MD trajectory and confirmed by ssNMR measurements (the distance restraints and the four dihedral angle restraints by PARIS-xy measurements and NHHC experiments, respectively).

<u>Hydrogen bond/Polar contact</u>

A2NH --- V4Hα

<u>Dihedral angle restraints</u>

Ψ,Φ G6
Ψ,Φ L7

<u>Distance restraints</u>

A3Cα --- Y8δ1
Y8δ1 --- L10Cγ
Y8ε1 --- L10Cγ

Supporting movie details

The full ssNMR-MD system from 0 – 330 ns with an increment of 30 ns is shown. More detailed trajectories are available upon request (m.h.weingarth@uu.nl or m.baldus@uu.nl). The file is in .pdb format and compressed as .tar.gz.

The movie provided is a fully modifiable .pdb file. For example, with Pymol, two short commands help to distinguish peptide and lipid residues:

i) to select the peptide:

select resi 1-20

ii) to select the lipids:

select resn dpo+lpo